Appendix 7

Sequential Magnetic Resonance Monitoring of Pulmonary Flow With Endovascular Stents Placed Across the Pulmonary Valve in Growing Swine

Titus Kuehne, MD; Maythem Saeed, DVM, PhD; Gautham Reddy, MD; Haydar Akbari, MD; Kelly Gleason, MD; Daniel Turner, MD; David Teitel, MD; Phillip Moore, MD; Charles B. Higgins, MD

Background—Patients with endovascular stent implantation for the treatment of right ventricular outflow tract obstruction are often left with incomplete relief of the obstruction and significant pulmonary regurgitation. A noninvasive and reproducible method for monitoring such patients is desirable. MRI in the presence of a stent, however, has to overcome the problem of potential metallic artifacts.

Methods and Results—Under x-ray fluoroscopic guidance, endovascular nitinol stents were placed across the pulmonary valve in 6 young pigs to induce pulmonary regurgitation. Five additional pigs served as controls. Initial MRI was performed after 2 days (13.5±1.8 kg) and follow-up after 3 months (32±2.9 kg). Pulmonary flow volumes and regurgitant fraction were quantified by velocity-encoded cine (VEC) MRI through (VEC-TS) and distal to (VEC-DS) the stent. VEC-TS was compared with VEC-DS and volumetric measurements of left and right ventricular stroke volumes provided by cine MRI ("gold standard"). Antegrade and retrograde pulmonary flow volumes by VEC-TS were slightly but significantly less than those with VEC-DS and cine MRI. Excellent correlations ($r>0.97$) for phasic pulmonary flow volumes as measured by VEC-TS and VEC-DS were shown. Pulmonary regurgitant fraction increased from 32.8±15% to 49.6±17% ($P<0.05$) over the course of 3 months with VEC-TS.

Conclusions—MRI demonstrates the progression of pulmonary regurgitation in growing swine. VEC MRI has the ability to quantify pulmonary blood flow inside the lumen of nitinol stents. MRI appears to be ideally suited for monitoring patients with endovascular nitinol stents in the pulmonary artery or pulmonary valve position. **(*Circulation*. 2001;104: 2363-2368.)**

Key Words: magnetic resonance imaging ■ stents ■ pulmonary heart disease

Pulmonary insufficiency is a frequent sequela after surgical or transcatheter treatment of obstruction of the right ventricular (RV) outflow tract and pulmonary artery. In addition, residual obstruction at the site of repair occurs frequently. Such isolated or combined chronic pressure and volume overload may cause irreversible RV failure.[1–3]

As an alternative to surgery, endovascular stents are rapidly gaining acceptance for the treatment of pulmonary artery and RV outflow tract obstruction.[4,5] Recent advances in technology have led to the placement of the first valved stent for the treatment of pulmonary insufficiency.[6] Although immediate and short-term results for the relief of pulmonary stenosis and insufficiency after stent and valved stent implantation are promising, little is known about their long-term effects.[7,8]

MRI appears to be ideally suited for monitoring pulmonary flow and ventricular function in patients.[9–13] MRI in the presence of a metallic stent is difficult, however, because of associated imaging artifacts. The paramagnetic properties of the materials and alloy design of the stent cause susceptibility artifacts at the stent wall and strongly reduce the signal-to-noise ratio inside the stent lumen.[14–17] Moreover, there have been no reports on the use of velocity-encoded cine (VEC) MRI in an in vivo model to quantify flow volumes and to assess flow profiles inside endovascular stents or stent grafts.

The aim of the present study was to use VEC MRI to (1) quantify pulmonary blood flow through and distal to a stent positioned over the pulmonary valve and (2) monitor progression in pulmonary regurgitant fraction in growing swine.

Methods

Stent Properties

Self-expanding nitinol stents (Memotherm, Angiomed) were used in the present study. The stents had a diameter of 18 mm and a length of 25 mm when fully expanded. With a (dimensionless) susceptibility value of 245×10^{-6}, nitinol is considered to be a weakly magnetic material. In MRI applications, nitinol experiences only slight forces and torques and produces limited image distortion and degradation.[18]

Received March 19, 2001; revision received July 9, 2001; accepted August 11, 2001.

From the Department of Radiology and the Division of Pediatric Cardiology, University of California, San Francisco.

Correspondence to Charles B. Higgins, MD, Department of Radiology, University of California San Francisco, 505 Parnassus Ave, L308, San Francisco, CA 94143-0628. E-mail charles.higgins@radiology.ucsf.edu

Circulation **is available at http://www.circulationaha.org**

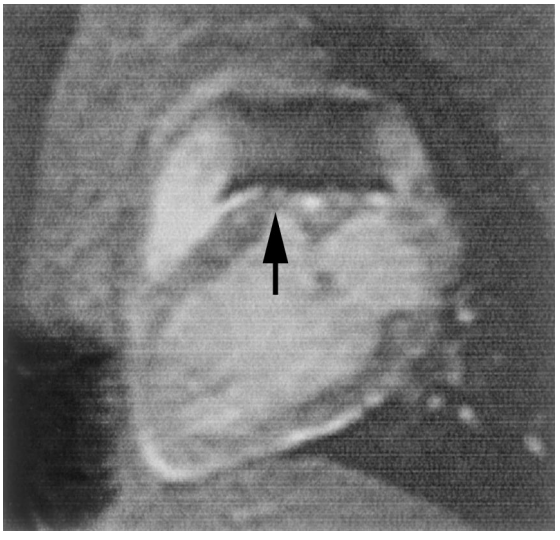

Figure 1. Representative double-oblique sagittal MR image showing position of nitinol stent across pulmonary valve (arrow).

Animal Model and Experimental Protocol

All procedures were performed in accordance with the National Institutes of Health's *Guide for Care and Use of Laboratory Animals* and with the approval of the Committee of Animal Research of the University. The animals were anesthetized with a mixture of telazol/ketamine/xylazine (0.025 mg/kg IM) for induction and 2% isoflurane for maintenance.

A total of 11 pigs were used in the present study. Five pigs served as control. In 6 pigs, stents were placed across the pulmonary valve (Figure 1) with a transcatheter technique under x-ray fluoroscopic guidance. A cine angiogram verified the position of the stent and the presence of pulmonary regurgitation. Two days after catheterization, the pigs underwent the initial MRI study. The same animals were restudied by MRI and x-ray angiography 3 months later. In all animals with stents, angiograms revealed pulmonary but no tricuspid insufficiency. After completion of the follow-up study, animals were euthanized with sodium pentobarbital (200 mg/kg IV), and the site and patency of the stents were examined. Between the initial and the follow-up studies, the animals gained weight, from 13.5±1.8 to 32±2.9 kg. One animal with a stent was excluded from the study because of infectious endocarditis resistant to antibiotic therapy.

MRI Techniques

ECG-gated MRI was performed with a 1.5-T MR imager (Signa 5, General Electric Medical Systems) with a standard body coil.

Pulmonary Flow Measurements and Stent Imaging

A VEC MR sequence was used in a double-oblique plane perpendicular to the dominating flow direction in the main pulmonary artery to measure forward (antegrade) and regurgitant (retrograde) flow volumes and flow velocities.[10] VEC MR images were acquired at 2 different sites in the main pulmonary artery, namely through the midportion of the stent (VEC-TS) and 2 to 3 mm distal to the stent (VEC-DS). VEC-DS images were performed beyond any susceptibility artifacts observed on the localizer images. The following acquisition parameters were used for VEC MRI: TR/TE 25/7 ms, slice thickness 5 mm, flip angle 30°, receiver bandwidth 31.25 kHz, field of view 24×24 cm, matrix 256×192, number of excitations (NEX) 2, and VEC 200 cm/s.

Ventricular Volume Measurements

Standard cine MRI in the cardiac short-axis plane was acquired to assess volumes of left ventricular (LV) and RV chambers.[11–13] The following imaging parameters were used: TR/TE 8/5 ms, slice thickness 10 mm, spacing 0, flip angle 20°, receiver bandwidth 31.25 kHz, field of view 24×24 cm, matrix 256×128, NEX 2, and 16 phases per cardiac cycle.

MR Image Analysis

Forward and regurgitant pulmonary flow volumes and peak flow velocity were measured by VEC-TS and VEC-DS imaging. For VEC-DS measurements, the velocity maps were obtained by manually tracing the main pulmonary artery contour on the magnitude images and then were applied to the phase images. For VEC-TS measurements, the contour of the stent was traced on both VEC magnitude images and VEC phase images, because the phase images showed less susceptibility artifact. Flow volume measurements of both methods for tracing the contour area were compared. There was 1.0±3.6% difference on the initial study and 1.3±2.1% difference on the follow-up study between the 2 methods. Measurements were not significantly different. Definition of the stent wall was found to be more unequivocal on VEC phase images, however; therefore, it was used in the calculation of flow volume measurements. Peak flow velocities were measured in the center of the stent and in the center of the pulmonary artery distal to the stent by use of a region of interest of 4 pixels on the VEC phase images.

Volumes obtained from cine MRI were used as "gold standard" to validate VEC-TS and VEC-DS measurements of pulmonary flow volumes. LV and RV stroke volumes were calculated as the difference between end-diastolic and end-systolic ventricular volumes. Cardiac outputs were calculated as the product of stroke volumes and heart rate. Pulmonary regurgitant volume was calculated as the difference between LV and RV outputs. After completion of all MRI studies, the position and morphology of the stents, including cross-sectional area, intimal wall thickening, and patency, were determined at autopsy.

Statistical Analysis

Data are presented as mean±SD. Two independent observers analyzed cine MR and VEC MRI. Interobserver and intraobserver variability was expressed as a percentage difference. Normal distribution of data was tested with the Kalmogorov-Smirnov test. Unpaired Student's *t* test and 1-way ANOVA with Scheffé's F test were used to determine the differences between the control and stented animals. Paired Student's *t* test was applied for comparison between acute and follow-up studies. A value of $P<0.05$ was considered significant. Linear regression analysis was used to determine the correlation between pulmonary flow volumes assessed with VEC-TS, VEC-DS, and cine MRI. Furthermore, the Bland-Altman test was performed to determine the agreement between the 3 MR methods measuring the same quantity.

Results

Pulmonary Flow Volumes

Control Group: Initial and Follow-Up Studies

In the control animals, there was no evidence of significant retrograde flow on VEC or cine MRI. Pulmonary forward flow volume measured by VEC MRI corresponded closely to that measured by cine MRI in both initial and follow-up studies. Analysis of the mean difference by Bland-Altman test disclosed maximal differences of $0.1\pm0.3\ L\cdot min^{-1}\cdot m^{-2}$ in the initial and $0.1\pm0.4\ L\cdot min^{-1}\cdot m^{-2}$ in the follow-up studies (Table 1). Regression analysis showed close correlation between the 2 methods ($r=0.93$ in the initial and $r=0.93$ in the follow-up study).

Insufficiency Group

Initial study: VEC-TS versus VEC-DS versus cine MRI: Pulmonary flow volumes as measured by VEC-TS were significantly smaller than with VEC-DS ($P<0.05$) but showed no significant difference from cine MRI (Table 1).

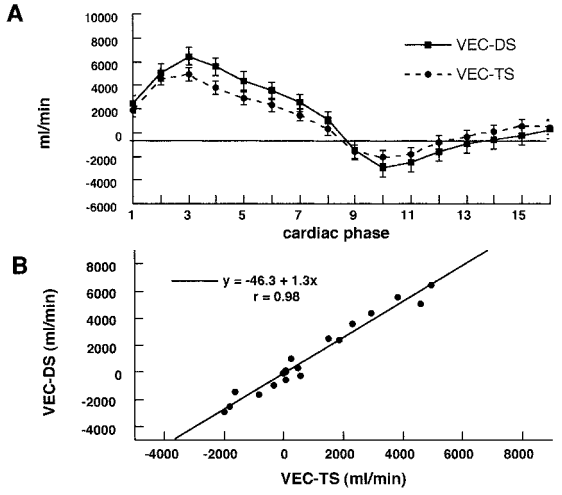

Figure 2. Pulmonary phasic flow pattern during 1 cardiac cycle measured through (VEC-TS) and distal to (VEC-DS) stent in initial study (A). Note close relationship between measurements obtained at the 2 sites (B).

Bland-Altman analysis demonstrated good agreement between the 3 methods, yielding, for pulmonary flow volume, only a underestimation of 0.9 ± 0.7 L · min^{-1} · m^{-2} for VEC-TS measurements compared with VEC-DS and 0.4 ± 0.4 L · min^{-1} · m^{-2} compared with cine MRI.

Figure 2A shows phasic pulmonary flow during 1 cardiac cycle as measured by VEC-TS and VEC-DS. Note the close flow pattern between the 2 measurements. Figure 2B demonstrates the close correlation between the 2 methods ($r=0.98$). Measurements for forward and retrograde pulmonary flow as measured by VEC-DS and cine MRI were not significantly different. The mean difference was 0.4 ± 0.8 L · min^{-1} · m^{-2}.

Follow-up study: VEC-TS versus VEC-DS versus cine MRI: Pulmonary flow volumes as measured by VEC-TS corresponded closely with VEC-DS and cine MR measurements. Flow volume as measured with VEC-TS was not significantly different from VEC-DS and cine MRI measurements (Table 1). Bland-Altman analysis showed good agreement between the applied methods, yielding, for pulmonary flow volume, a underestimation of only 0.6 ± 0.5 L · min^{-1} · m^{-2} for VEC-TS measurements compared with VEC-DS and 0.4 ± 0.6 L · min^{-1} · m^{-2} compared with cine MRI. Figure 3A shows the pattern of phasic pulmonary flow during 1 cardiac cycle as measured by VEC-TS and VEC-DS. Figure 3B demonstrates the good correlation between the 2 methods ($r=0.97$). Measurements for forward and retrograde pulmonary flow as measured by VEC-DS and cine MRI were not significantly different. The mean difference was negligible (0.1 ± 0.6 L · min^{-1} · m^{-2}).

Sequential Monitoring of Pulmonary Regurgitation

Stent placement across the pulmonary valve caused severe pulmonary regurgitation. A significant ($P<0.05$) increase in regurgitant volume and fraction was documented in all animals over the course of 3 months (Table 1). The mean regurgitant fraction increased from $32.8\pm15.0\%$ to $49.6\pm17.0\%$ when measured with VEC-TS, from $35.1\pm12.5\%$ to $52.2\pm16.4\%$ when measured with VEC-DS, and from $30.2\pm5.6\%$ to $50.6\pm8.9\%$ when measured with cine MRI.

Pulmonary regurgitant fraction as measured by VEC-TS compared with VEC-DS and cine MRI correlated closely. Bland-Altman analysis showed good agreement between the 3 methods in the early and the follow-up studies (Figure 4). The correlation between regurgitant fraction as measured by VEC-TS and VEC-DS and between VEC-TS and cine MRI were good in the initial ($r=0.90$, $r=0.74$, respectively) and in the follow-up studies ($r=0.99$, $r=0.81$, respectively). For all measurements, interobserver variability was 3.1% for VEC MRI and 5.7% for cine MRI, and intraobserver variability was 2.5% for VEC MRI and 3.7% for cine MRI.

Pulmonary Phasic Flow Profile and Stent Morphology

In the control group, peak flow velocity was 74 ± 5 cm/s in the initial study and 79 ± 9 cm/s in the follow-up study (Table 2). The mean cross-sectional area of the pulmonary artery, measured by VEC MRI during the same cardiac phase as the corresponding peak flow velocity, increased ($P<0.001$) from 194 ± 22 mm^2 in the initial study to 395 ± 48 mm^2 in the follow-up study.

In the initial study of the insufficiency group, peak flow velocity was 59 ± 11 cm/s as measured by VEC-TS and 71 ± 9 cm/s as measured by VEC-DS ($P<0.05$) (Table 2). The cross-sectional area of the stent (219 ± 18 mm^2) was larger

TABLE 1. Measurements of Pulmonary Flow Volume and Regurgitant Fraction in Control and Stented Animals

	Forward Flow		Regurgitant Flow		Regurgitant Fraction, %	
	Stented	Control	Stented	Control	Stented	Control
Initial study						
VEC-TS	4.2±1.4*	NA	1.2±0.2	NA	32.8±15.0	NA
VEC-DS	4.9±1.1	4.6±0.5	1.6±0.3	0	35.1±12.5	0
Cine MRI	4.7±0.6	4.4±0.5	1.4±0.3	0.03±0.1	30.2±5.6	0.7±0.5
Follow-up study						
VEC-TS	4.3±0.8	NA	2.0±0.5	NA	49.6±17.0†	NA
VEC-DS	4.6±0.9	4.5±0.5	2.3±0.5	0	52.2±16.4†	0
Cine MRI	4.4±0.8	4.7±0.6	2.2±0.1	0.04±0.4	50.6±8.9†	0.9±0.8

Flow volume measurements are listed as mean±SD (L · min^{-1} · m^{-2}). *$P<0.05$ compared to VEC-DS, †$P<0.05$ compared to initial study.

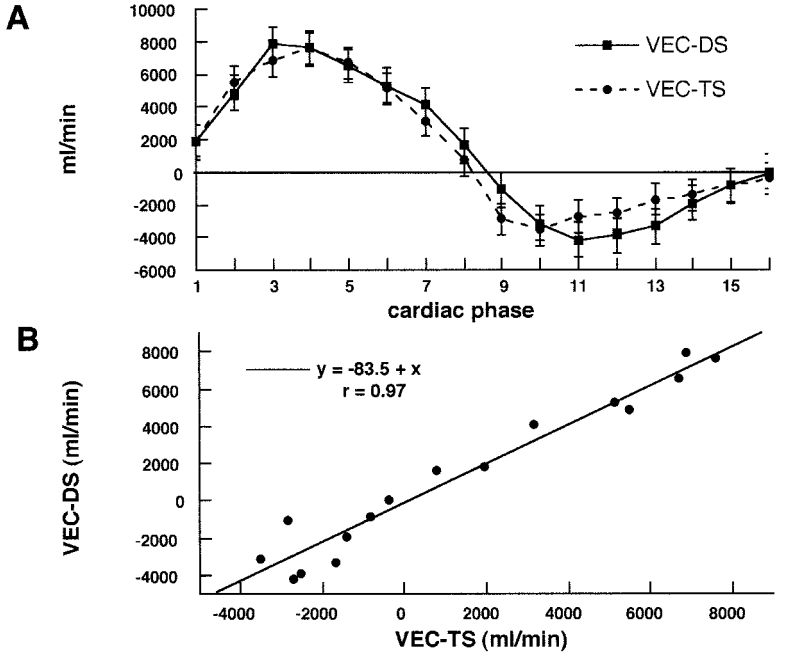

Figure 3. Pulmonary phasic flow pattern during 1 cardiac cycle measured through (VEC-TS) and distal to (VEC-DS) stent in follow-up study (A). Note close relationship between measurements obtained at the 2 sites (B).

than the cross-sectional area of the pulmonary artery distal to the stent (185±23 mm^2) ($P<0.05$). In the follow-up study, the mean cross-sectional area of the stent remained the same as in the initial study (225±12 mm^2). The pulmonary artery distal to the stent, however, was significantly dilated (510±71 mm^2) ($P<0.001$). In concordance with this, a higher peak flow velocity of 124±24 cm/s was measured inside the stent compared with a peak velocity of 40±9 cm/s in the distal pulmonary artery ($P<0.001$).

The cross-sectional surface area of the stent was sharply demarcated on VEC phase images. Antegrade and retrograde pulmonary flow were clearly visualized over the entire stent lumen on phase images (Figure 5). A 1- to 2-pixel-wide ring of artifact defined the wall of the stent. Conversely, the VEC magnitude images showed wider susceptibility artifact from the stent, with a width of 4.0±1.9.

The surface area of the stent lumen, determined at the follow-up study on VEC phase images, corresponded closely with measurements determined at autopsy (225±12 and 227±9 mm^2, respectively, $r=0.96$) (Table 2). At autopsy, the nitinol stents were unobstructed and showed only a thin layer of endothelium, with no appreciable intimal thickening (Figure 6).

Discussion

The present study demonstrates that pulmonary flow measurements by VEC MRI, acquired through endovascular nitinol stents, correspond closely with VEC MRI acquired distal to the stent or volumetric measurements of the cardiac ventricles provided by cine MRI. Cine MRI of the ventricles is totally independent of artifacts due to the stent and serves as a validating technique ("gold standard"). These results imply that VEC MRI is an effective, noninvasive method to

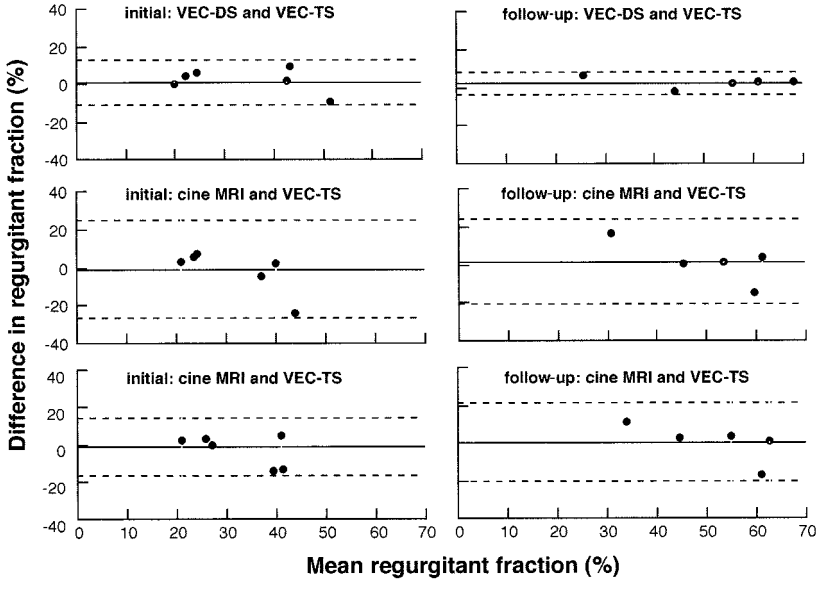

Figure 4. Plots show agreements between methods used to measure pulmonary regurgitant fraction. Left, Initial study; right, follow-up study. Bland-Altman analysis showed close agreement between cine MRI, VEC-TS, and VEC-DS.

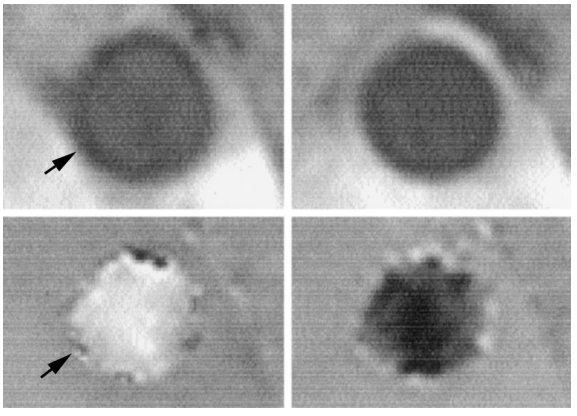

Figure 5. VEC MR magnitude and phase images acquired during mid systole (left) and mid diastole (right) through nitinol stent. Note susceptibility artifacts derived from stent wall (arrow, top left) and reduced signal-to-noise ratio in lumen of stent on magnitude image. Conversely, stent wall is well defined on phase images (arrow, bottom left), and flow is visualized over entire stent lumen. Antegrade flow appears as bright signal (bottom left), retrograde flow as dark signal (bottom right).

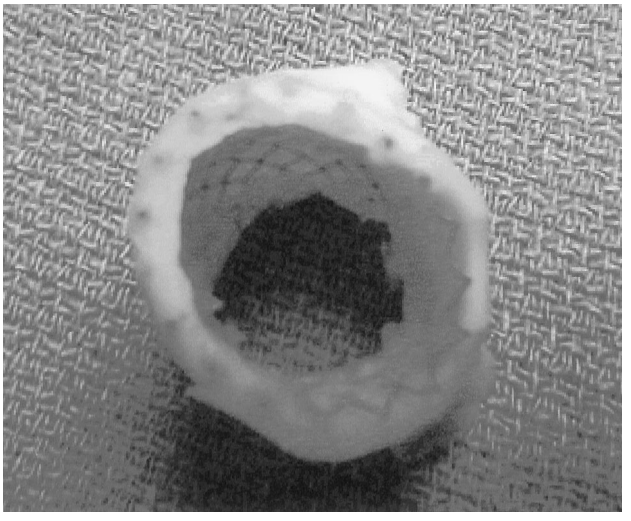

Figure 6. Image of nitinol stent at autopsy 3 months after placement across pulmonary valve. Stent is covered by thin layer of endothelium. Stent lumen was not obstructed by intimal hyperplasia or thrombus.

quantify pulmonary flow volume and regurgitant fraction in patients with a nitinol stent in the pulmonary valve, pulmonary artery, or pulmonary conduit position. In addition, the severe increase of regurgitant fraction over time and with growth of the animals emphasizes the clinical importance of monitoring patients with pulmonary insufficiency, with the intent of preventing irreversible myocardial dysfunction as a consequence of increasing volume overload.

An in vitro study has assessed the error of VEC MRI for measuring blood flow in the presence of stainless steel coronary stents.[19] In this study, a significant decrease in flow velocity measurements was noted when measured near the stent. In stents with material properties yielding high magnetic susceptibility, phase offset phenomena apparently reduce flow measurements significantly. As shown in the present study, however, in the presence of nitinol stents with relatively large surface areas, flow volume measurements were reasonably accurate. In addition, qualitative flow phenomena were detectable over the entire luminal surface area of the nitinol stents, even in the region adjacent to the wall of the stent. Antegrade and retrograde pulmonary flow were directionally encoded on the VEC phase images (Figure 5). This observation supports the notion that phase information of the moving spins is not degraded within the nitinol stent lumen.

On VEC phase images, the nitinol stent wall was sharply defined, and no image distortion due to susceptibility artifacts was noted (Figure 5). A possible explanation is the compensation in velocity maps for spin frequency offset phenomena, which are caused by local field inhomogeneities due to susceptibility. In contrast, definition of the nitinol stent wall was more ambiguous on the VEC magnitude because of susceptibility artifacts (Figure 5).

In addition, the present study demonstrates that 3 months after stent placement, significant hemodynamic and morpho-

TABLE 2. Body Weight, Heart Rate, Cardiac Output, Peak Flow Velocity, and Cross-Sectional Area of the Pulmonary Artery in Control and Stented Animals

	Control Group		Stented Group	
	Initial Study	Follow-Up Study	Initial Study	Follow-Up Study
Weight, kg	13.3±1.2	33±2.1	13.9±1.8	30±3.3
Heart rate during MRI sessions	97±10	79±7	93±9	84±6
RV cardiac output, L/min	1.7±0.5	3.4±0.6	1.9±0.4	3.0±0.5
Peak flow velocity, cm/s				
Distal main pulmonary artery	74±5	79±9	71±9	40±9
Inside the stent	NA	NA	59±11	124±24
Cross-sectional area, mm^2				
Distal main pulmonary artery at MRI	194±22	395±51	185±23	510±71†
Stent at MRI	NA	NA	219±18*	225±12
Stent at autopsy	NA	NA	NA	227±9

Measurements are listed as mean±SD. RV cardiac outputs were measured with cine MRI. Peak flow velocities and cross-sectional area were measured with VEC MRI. Measurements were acquired during mid systole. The cross-sectional areas of the stents were assessed with MRI and at autopsy. *$P<0.05$ compared to cross-sectional area distal to main pulmonary artery; †$P<0.001$ compared to initial study and TS.

logical differences between the stented and nonstented sections of the pulmonary artery occur (Table 2). With animal growth, the tube-like stented section of the pulmonary artery remained at its original size. Consequently, the increased cardiac output that occurred with growth of the animals caused peak flow velocities inside the stent to increase from 59±11 to 124±24 cm/s. High flow velocities in the presence of a stent with reduced distensibility and high shear stress most likely cause considerable flow turbulence. Furthermore, the large dimension and high distensibility of the nonstented distal pulmonary artery may serve in the adult animals as a capacitor for inflowing and backflowing blood. This has to be taken into account when comparing VEC-DS with VEC-TS measurements on late follow-up studies.

Because both magnetic susceptibility artifacts and turbulent flow are potential sources of intravoxel dephasing and signal loss and may lead to errors in quantitative flow measurements, methods must be explored to minimize the echo time of pulse sequences and thus the time available for spin dephasing. Future research will need to investigate in a systematic manner the effect of (1) stent size, material, and geometry; (2) the orientation of the stent toward the main magnetic field; and (3) the effect of contrast media on VEC MRI measurements and stent patency.

One common clinical problem of intravascular stents is the high incidence of restenosis. It would be desirable to evaluate stent patency noninvasively. At present, however, most clinically available stents reduce or vitiate signal within the stent on MR images. The design of the available stents prevents MR radiofrequency pulses from penetrating the wire mesh of the stent, leading to a reduction of MR signal inside the stent lumen.[14,20] In addition, susceptibility artifacts are superimposed on the stented vascular wall.

Both in vitro and in situ studies[21] have demonstrated close agreement between Doppler sonography, cardiac catheterization, and VEC MRI for quantification of vascular stenosis. It will be important to determine in future studies whether monitoring of flow through different stents can be used to detect and quantify stent stenosis.

Study Limitations

In the present study, only nitinol stents with a diameter of 18 mm, when freely expanded, were evaluated. Although stents of such size are often anticipated in young patients with congenital heart diseases, they are indicated in a variety of adult patients with congenital heart diseases or acquired diseases of the aorta. The data obtained in this study cannot be extrapolated to stents of different sizes or types. It should be noted that radiofrequency shielding effects of the stent wall due to eddy currents depend mainly on the inherent design of the stent and, to a lesser extent, on the stent diameter.[15,20] Moreover, the degree of image distortion due to susceptibility artifacts is related to the thickness of the paramagnetic material.[18] In smaller stents, the thickness of the stent alloy is often less than in larger stents, suggesting that quantitative flow analysis by VEC MRI may be feasible within small endovascular stents. Additional research will be necessary, however, to establish this.

Conclusions

This MR study demonstrates the progression of pulmonary regurgitation in growing swine. VEC MRI has the ability to quantify pulmonary blood flow inside the lumen of nitinol stents. MRI appears to be ideally suited for noninvasively monitoring patients with nitinol stents in the pulmonary artery or pulmonary valve position.

References

1. Therrien J, Siu SC, McLaughlin PR, et al. Pulmonary valve replacement in adults late after repair of tetralogy of Fallot: are we operating too late? *J Am Coll Cardiol*. 2000;36:1670–1675.
2. Schamberger MS, Hurwitz RA. Course of right and left ventricular function in patients with pulmonary insufficiency after repair of tetralogy of Fallot. *Pediatr Cardiol*. 2000;21:244–248.
3. Murphy JG, Gersh BJ, Mair DD, et al. Long-term outcome in patients undergoing repair of tetralogy of Fallot. *N Engl J Med*. 1993;329: 593–599.
4. Powell AJ, Lock JE, Keane JF, et al. Prolongation of RV-PA conduit life span by percutaneous stent implantation: intermediate-term results. *Circulation*. 1995;92:3282–3288.
5. Hosking MC, Benson LN, Nakanishi T, et al. Intravascular stent prosthesis for RV outflow obstruction. *J Am Coll Cardiol*. 1992;20:373–380.
6. Bonhoeffer P, Boudjemline Y, Saliba Z, et al. Transcatheter implantation of a bovine valve in pulmonary position. *Circulation*. 2000;102:813–816.
7. Cheung YF, Sanatani S, Leung MP, et al. Early and intermediate-term complications of self-expanding stents limit its potential application in children with congenital heart disease. *J Am Coll Cardiol*. 2000;35: 1007–1015.
8. O'Laughlin MP, Slack MC, Grifka RG, et al. Implantation and intermediate-term follow-up of stents in congenital heart disease. *Circulation*. 1993;88:605–614.
9. Helbing WA, de Roos A. Clinical applications of cardiac magnetic resonance imaging after repair of tetralogy of Fallot. *Pediatr Cardiol*. 2000;21:70–79.
10. Rehbergen SA, Chin JGJ, Ottenkamp J. Pulmonary regurgitation in the late postoperative follow-up of tetralogy of Fallot. *Circulation*. 1993;88: 2257–2266.
11. Helbing WA, Rebergen SA, Maliepaard C, et al. Quantification of RV function with magnetic resonance imaging in children with normal hearts and with congenital heart disease. *Am Heart J*. 1995;130:828–837.
12. Rominger MB, Bachmann GF, Pabst W, et al. RV volumes and ejection fraction with fast cine MRI in breath-hold technique: applicability, normal values from 52 volunteers, and evaluation of 325 adult cardiac patients. *J Magn Reson Imaging*. 1999;10:908–918.
13. Semelka RC, Tomei E, Higgins C, et al. Normal LV dimensions and function: interstudy reproducibility of measurements with cine MRI. *Radiology*. 1990;174:763–768.
14. Klemm T, Duda S, Machann J, et al. MRI in the presence of vascular stents: a systematic assessment of artifact for various stent orientations, sequence types, and field strengths. *J Magn Reson Imaging*. 2000;12:606–615.
15. Lehnhart M, Voelk M, Nitz WR, et al. Stent appearance at contrast-enhanced MR angiography: in vitro examination with 14 stents. *Radiology*. 2000;217:173–178.
16. Hilfiker PR, Quick HH, Debatin JF. Plain and covered stent-grafts: in vitro evaluation of characteristics at three-dimensional MR angiography. *Radiology*. 1999;211:693–697.
17. Link J, Steffens JC, Brossmann J, et al. Iliofemoral arterial occlusive disease: contrast-enhanced MR angiography for preinterventional evaluation and follow-up after stent placement. *Radiology*. 1999;212:371–377.
18. Schenck JF. The role of magnetic susceptibility in magnetic resonance imaging: MRI magnetic compatibility of the first and second kinds. *Med Phys*. 1996;23:815–851.
19. Lethimonnier F, Bouligand B, Thouveny F, et al. Error assessment due to coronary stents in flow-encoded phase contrast MR angiography: a phantom study. *J Magn Reson Imaging*. 1999;10:899–902.
20. Haacke M, Brown RW, Thompson MR, et al. *Magnetic Resonance Imaging: Physical Principles and Sequence Design*. New York, NY: Wiley-Liss, John Wiley & Sons Publication; 1996.
21. Gutberlet M, Boeckel T, Hosten N, et al. Arterial switch procedure for D-transposition of the great arteries: quantitative midterm evaluation of hemodynamic changes with cine MRI and phase-shift velocity mapping-initial experience. *Radiology*. 2000;214:467–475.